21st Australasian Fluid Mechanics Conference
Adelaide, Australia
10-13 December 2018

Energy Harvesting of Two Inverted Piezoelectric Flags in Tandem Arrangement

S. Mazharmanesh[1], J.Young[1], F.-B. Tian[1] and J.C.S. Lai[1]

[1]School of Engineering and Information Technology
University of New South Wales Canberra, ACT 2600, Australia

Abstract

The interaction of two tandem inverted piezoelectric flags in uniform flow is investigated. An immersed boundary method based on the multi-block lattice Boltzmann method (LBM) is used to study the dynamics of the fluid-structure interaction of the tandem flags as well as their energy harvesting performance. At a Reynolds number of 100, mass ratio 2.9 and bending rigidity 0.26, we consider two values for the piezo-mechanical coupling parameter (α) and five values for the piezoelectric tuning parameter (β) and vary the streamwise gap distance (G_x/L) from 0.1 to 3.2 to study hydrodynamic and electrodynamic responses of the inverted flags. It is found that the power coefficient of the tandem inverted flags varies with β. Based on the power coefficient, the optimum values of β for both flags are found at each streamwise gap distance and α. The results show that with increasing α in each streamwise gap, the optimum value of β increases. In addition, the power coefficient changes with the streamwise gap distance. The maximum one occurs at $G_x/L = 1.8$ which is attributed to the constructive interaction effect between vortices shed from the flags.

Introduction

The interaction between a viscous incompressible fluid and a flexible structure is ubiquitous in nature such as a flag flapping in the air. Flow induced vibration of immersed flexible structures has been studied extensively because of its fundamental importance and potential applications in engineering. Researchers found that flow induced vibration could be useful in many applications such as energy harvesting [13]. Flexible structures were applied to harvest energy. This type of energy harvester is able to generate electric energy from fluid currents which are ubiquitous in nature without contaminating the surroundings. Among the energy harvesters based on flexible structures, the flexible plate harvester has attracted growing attention because it could vibrate continuously at very low speeds [3,5]. The flexible plate harvester consists of flexible plates covered with piezoelectric materials, producing electricity through two energy conversion processes. First, the flow energy is converted to mechanical energy of the flexible plate. Second, piezoelectric materials attached to the flexible plate convert the mechanical energy of the plate to electrical energy that powers a resistive output circuit. [2,10]. Research has shown that most of the energy waste happens during conversion of the fluid flow energy into mechanical energy of the plates [1]. Therefore, several studies focused on different approaches to improve the efficiency of this conversion process. Kim et al [7] proposed an inverted flag with a free leading edge and a clamped trailing edge. They showed that the inverted flag is more unstable than the conventional flag clamped at the leading edge. As a result, the inverted flag flaps with larger amplitude even with a lower incoming flow velocity. Furthermore Shoele & Mittal [14] investigated an inverted flag coupled with piezoelectric materials numerically at Reynolds number $Re = 200$. They indicated that the peak of electrical energy efficiency for the conventional flag is approximately an order of magnitude lower than that for the corresponding inverted flag.

Hydrodynamic interaction among multiple flags may improve energy harvesting performance of the flags. Some studies have been conducted to evaluate the interaction between the conventional flags in the tandem arrangement [6,8,12,20]. These studies show that the stability of the system is determined by Re and distances between the flags. Moreover, the amplitude of the downstream flag is larger when both flags flap. The difference between the drag of the upstream and downstream flags is explained by the vortex structures in the wake of multiple flags [8]. Vortices merge either constructively or destructively. Very recently, Huang et al. [4] numerically studied two tandem inverted flags at $Re = 200$ by varying the streamwise gap distance. They found that for the simple tandem configuration, the amplitude of the downstream flag is smaller than that of the upstream flag.

In the studies of tandem inverted flags, the coupling with the piezoelectric mechanism is not considered. Therefore, these studies cannot quantify the energy harvesting performance directly and determine the effect of piezoelectric materials on the dynamics of the flag. In this work we study the flow induced vibration characteristics and energy extraction performance of two inverted flags coupled with the piezoelectric materials in a uniform flow by using the immersed boundary-lattice Boltzmann method [15]. The hydrodynamic interaction among the two flags is explored with a focus on energy extraction enhancement.

Physical Problem and Governing Equations

As shown in figure 1, the configuration consists of two inverted flags with their leading edges free to flap and their trailing edges clamped. The length of the flags is L and they are subjected to a uniform flow with velocity U.

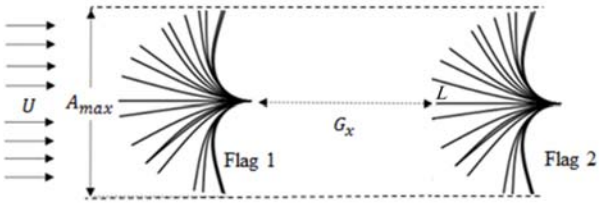

Figure 1: Schematic of the two tandem inverted flags in uniform flow.

The fluid is governed by the continuity equation and the incompressible Navier–Stokes equations:

$$\nabla\cdot\mathbf{u}=0, \quad \rho_f\left(\frac{\partial\mathbf{u}}{\partial t}+\mathbf{u}\cdot\nabla\mathbf{u}\right)=-\nabla p+\mu_f\nabla^2\mathbf{u}, \qquad (1)$$

where $\boldsymbol{u}$ is the velocity vector. The inverted flag dynamics is governed by the following equation

$$m_s \frac{\partial^2 \mathbf{X}}{\partial t^2} = \frac{\partial}{\partial s}\left(E_s\left(\left|\frac{\partial \mathbf{X}}{\partial s_0}\right| - 1\right)\frac{\partial \mathbf{X}}{\partial s}\right) - \frac{\partial^2}{\partial s^2}\left(E_B \frac{\partial^2 \mathbf{X}}{\partial s^2}\right) + \mathbf{F}, \quad (2)$$

where $\boldsymbol{X}(s)$ is the position of the inverted flag, s is arc length along the flag, s_0 is the arc length at the unstretched state, m_s is linear density, E_B is bending rigidity, E_s is the stretching coefficient and $\boldsymbol{F}$ is hydrodynamic traction per unit length. The trailing edges of both flags are fixed that the boundary conditions are given by

$$\mathbf{X} = \mathbf{X}_0, \quad \frac{\partial \mathbf{X}}{\partial s} = (-1, 0), \quad (3)$$

where $\boldsymbol{X}_0$ is the location of the clamped edge. At the free leading edge ($s = L$), the boundary conditions are

$$\frac{\partial^2 \mathbf{X}}{\partial s^2} = 0, \quad \frac{\partial^3 \mathbf{X}}{\partial s^3} = 0. \quad (4)$$

The coupled fluid-structure system is governed by four non-dimensional parameters: mass ratio m^*, non-dimensional bending coefficient B, Reynolds number Re and non-dimensional stretching coefficient S, defined by

$$m^* = m_s/\rho_f L, \quad B = E_B/\rho_f U^2 L^3, \quad Re = \rho_f UL/\mu_f,$$
$$S = E_s/\rho_f U^2 L^2. \quad (5)$$

In this study $m^* = 2.9$, $B = 0.26$ and $Re = 100$ are used in the simulations. These parameters are chosen based on the fact that these values lead to the maximum flapping amplitude for a single inverted flag without coupling with piezoelectric materials [7].

Following [10], we assume that both surfaces of the flag are covered with very small piezoelectric patches with segmentation lengths much smaller than L. In addition, a purely resistive circuit is considered at the output. The governing equations for piezoelectric-structure coupling are given by

$$Q(s,t) = cV + \psi \frac{\partial^2 \mathbf{X}}{\partial s^2}, \qquad \frac{\partial Q}{\partial t} + \frac{1}{R}V = 0,$$
$$M(s,t) = E_b \frac{\partial^2 \mathbf{X}}{\partial s^2} - \psi V. \quad (6)$$

where Q is charge transfer per unit length, V is electric voltage, c is linear capacitance of the piezoelectric element, ψ is coupling coefficient related to the intrinsic material properties of piezoelectric patches, R is resistance of a purely resistive circuit and M is total bending moment along the flag.
In addition to the four non-dimensional parameters in equation (5), two new non-dimensional parameters are defined to characterize the coupled fluid-structure-electrical system:

$$\alpha = \psi/\sqrt{E_b c}, \qquad \beta = RcU/L. \quad (7)$$

α is piezo-mechanical coupling parameter and dependent on the piezoelectric material characteristics. It is a function of capacitance and resistance to bending. β is piezoelectric tuning parameter and represents the non-dimensional electric loads in the electric circuit.
The power harvested by the piezoelectric flags is quantified based on the instantaneous power dissipated in the piezo patches and normalized with $\rho_f U^3 L^2$. Therefore, the electric power coefficient is computed by

$$C_P = \left(\frac{1}{R}\int_0^L V^2 ds\right)/\left(\rho_f U^3 L^2\right). \quad (8)$$

An immersed boundary method based on the multi-block lattice Boltzmann method (LBM) [15] is employed to solve the fluid-structure-electric interaction system. In this method, the fluid dynamics described by Eq. (1) is obtained by using the multi-block lattice Boltzmann method, which has attracted growing attention in the recent years due to its high computational efficiency and low numerical dissipation [11]. In this work, we use D2Q9 (the nine-velocity model in two dimensions) LBM model. The structural dynamics is solved by using the finite difference method as detailed in [16]. The electrical equations are also solved by using the finite difference method. The fluid-structure interaction is achieved by the immersed boundary method in which the stress exerted by the structure on the fluid is spread onto the ambient fluid nodes near the flag. Details of the method used have been given in the references mentioned, and thus are not repeated here. The solver used in this work has been validated and verified in our previous works [9,17,18,19].

Results and Discussion

For two inverted flags, the computational domain is a rectangular box of $42L \times 22L$ in size with approximately 2.1×10^5 cells. The minimum mesh size around the flags is $0.0125L$ in both x- and y-directions. The non-dimensional time step for the block around the flags is $\Delta tU/L = 0.0005$. A uniform grid with 160 points is used to discretise each flag.

In order to investigate the hydrodynamic interaction of the two tandem inverted flags, the streamwise gap separation distance G_x/L is varied from 0.1 to 3.2 while all the other variables are constant. The piezo-mechanical coupling parameter α is dependent on the piezo material characteristics. Widely available piezoelectric materials such as PZT (lead zirconate titanate) exhibit $\alpha = 0.3$ and 0.5 [10]. Therefore, we test the performance of the tandem inverted flags for these values of α.

The relation between harvested power and piezoelectric tuning parameter β is shown in figure 2. $\bar{C}_P$ is the time average of the power coefficient calculated over a period of approximately last 15 flapping cycles of the 35 cycles in the simulation.

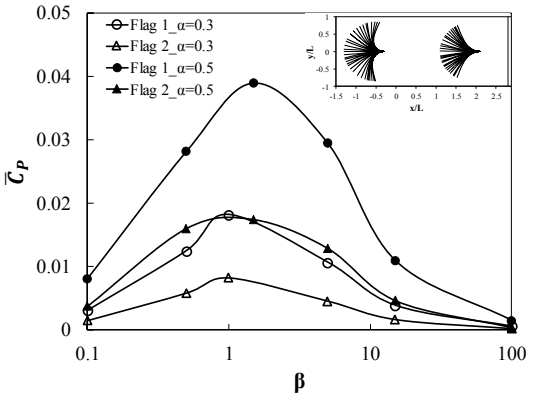

Figure 2. Time average of power coefficient $\bar{C}_P$, at $G_x/L = 1.4$.

As expected, there is a peak in the $\bar{C}_P$ curve. When $\beta \ll 1$ and $\beta \gg 1$ the resistance acts as a short circuit or open circuit, respectively. In both cases, no energy is dissipated and $\bar{C}_P = 0$. The maximum $\bar{C}_P$ occurs at $\beta = 1$ when $\alpha = 0.3$ and at $\beta = 1.5$ when $\alpha = 0.5$. As the variation of $\bar{C}_P$ with β is similar for different streamwise gap separation distances G_x/L, only one separation distance G_x/L, =1.4 is plotted here. As shown in figure 2, the deformation pattern of the tandem flags indicate symmetric flapping of the two flags in the first mode of bending.

Figure 3 exhibits the effects of adding piezoelectric coupling on the flapping performance of the flags. $\alpha = 0$ denotes no

piezo coupling. Firstly, for all G_x/L the amplitude of Flag 2 is smaller than that of Flag 1 because the downstream flag is flapping in the wake of the upstream flag where the available flow energy is lower than in the free stream.

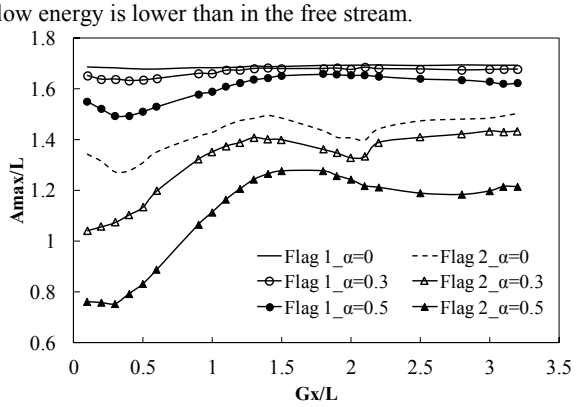

Figure 3. Evolution of peak-to-peak flapping amplitude of the leading edge, A_{max}/L.

Furthermore, it can be seen that adding piezoelectric material to the flags decreases the flapping amplitude which decreases with increasing α because increasing α increases the rigidity of the flag. On the other hand, increasing α provides a feasibility to more elastic energy in the flags is converted to electrical energy.

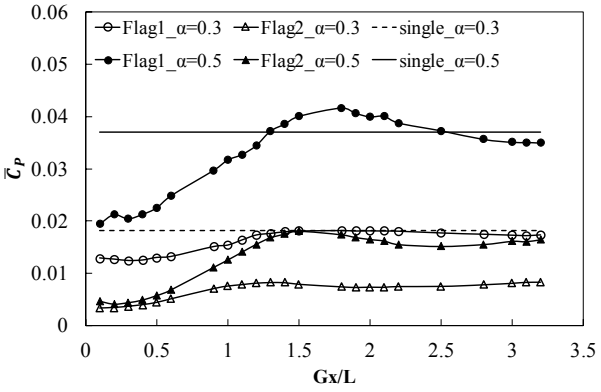

Figure 4. Evolution of power coefficient $\bar{C}_P$, at $\beta = 1$ (solid fill) and $\beta = 1.5$ (no fill)

Figure 4 shows the variation of $\bar{C}_P$ with G_x/L, at $\beta = 1$ and $\beta = 1.5$ for $\alpha = 0.3$ and $\alpha = 0.5$, respectively. It can be seen that for both flags, increasing α increases $\bar{C}_P$ particularly for $G_x/L > 1$ where $\bar{C}_P$ of Flag 2 for $\alpha = 0.5$ approaches that of Flag 1 for $\alpha = 0.3$. Since Flag 1 has higher flapping amplitude than Flag 2, $\bar{C}_P$ of Flag 1 is greater than that for Flag 2 for both values of α. Generally, $\bar{C}_P$ curves follow A_{max}/L curves regarding to the variation of G_x/L. For $\alpha = 0.3$ $\bar{C}_P$ of both flags increases gradually with increasing G_x/L up to $G_x/L = 1.4$ where $\bar{C}_P$ of Flag 1 reaches the value of the single flag ($\bar{C}_P = 0.0107$). Then it remains almost constant with increasing G_x/L for both flags. Due to this fact that in this streamwise gap distance ($G_x/L = 1.4$) the flapping amplitudes of both flags are maximum, the maximum of $\bar{C}_P$ occurs in this distance. For $\alpha = 0.5$ Flag 1 exhibits a peak at $G_x/L = 1.8$ ($\bar{C}_P = 0.0416$) while Flag 2 has a peak at $G_x/L = 1.5$ ($\bar{C}_P = 0.0181$). Before the peak points, $\bar{C}_P$ of both flags grows sharply with increasing G_x/L whereas after the peak points $\bar{C}_P$ decreases slowly. For comparison, the maximum $\bar{C}_P$ of a conventional flag with clamped leading edge in $\alpha = 0.5$ is ≈ 0.00325 [10] which is much smaller than the maximum $\bar{C}_P$ of inverted flags. Interestingly, for $\alpha = 0.5$ $\bar{C}_P$ of Flag 1 becomes greater than that of the single flag for $1.3 < G_x/L < 2.5$. This phenomenon can be explained by the change in the flapping frequency. As shown in figure 5 for $\alpha = 0.5$ at approximately $1.3 < G_x/L < 2.5$, the frequencies of both flags are greater than that of the single flag. As a result, the frequency of the flag bending and formation of the leading-edge vortex increases and consequently more mechanical energy is stored in the flags. Although at $\alpha = 0.3$ and $1.2 < G_x/L < 2.0$ the frequency of the tandem flags is higher than the frequency of single flag, the lower amount of α causes $\bar{C}_P$ of Flag 1 does not exceed the power coefficient of the single flag.

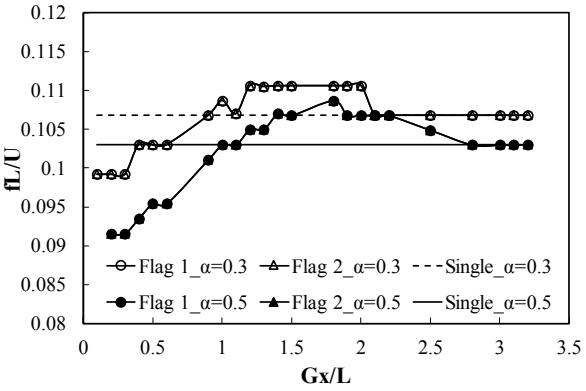

Figure 5. Evolution of non-dimensional frequency fL/U, at $\beta = 1$ (solid fill) and $\beta = 1.5$ (no fill)

A constructive interaction mode between vortices causes the increase in the flag's flapping frequency. This occurs when vortices rotating in the same sense encounter each other, merge and produce a larger vortex. This is illustrated in Figure 6 (a) which displays the instantaneous vorticity counters for $\alpha = 0.5$ and $G_x/L = 1.8$. The red vortices are counterclockwise and the blue vortices are clockwise. The counterclockwise vortex (A) which sheds from the leading edge of Flag 2 encounters the counterclockwise vortex (B) which sheds from Flag 1. They merge constructively and enhance the performance of both flags so that the maximum flapping amplitude and as well the maximum $\bar{C}_P$ of the flags occur at this separation distance. For both α, when G_x/L is smaller than one, the destructive interaction mode is observed. In the destructive mode two counter-rotating vortices encounter each other, leading to both amplitude and drag force decreasing. This is illustrated in Figure 6 (b) which displays instantaneous vorticity contours for $\alpha = 0.5$ and $G_x/L = 0.5$. The counterclockwise vortex (A) which sheds from the leading edge of Flag 2 encounters with the clockwise vortex (B) which sheds from Flag 1. They annihilate each other, reducing the flapping amplitude of both flags. As G_x/L decreases further, the destructive mode becomes stronger. It should be noted that, although there are constructive interaction modes for some G_x/L, the flapping amplitude of Flag 2 is always smaller than that of Flag 1. In fact, the reduction of available energy caused by the upstream flag (Flag 1) dominates the enhancement caused by the constructive mode. Therefore, Flag 2 flaps with a smaller amplitude than Flag 1.

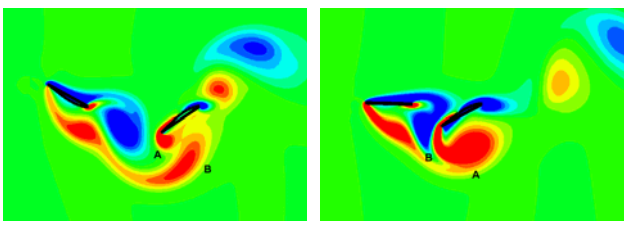

(a) $G_x/L = 1.8$ (b) $G_x/L = 0.5$

Figure 6. Instantaneous vorticity counter for $\alpha = 0.5$.

Conclusions

The energy harvesting performance of two tandem inverted piezoelectric flags in uniform flow is numerically investigated in this work. The inverted flags have clamped trailing edges and free leading edges. Both surfaces of the flags are covered with piezoelectric patches which convert mechanical energy into electrical energy powering purely resistive output circuits. An immersed boundary method based on the multi-block lattice Boltzmann method (LBM) is employed to solve the fluid-structure-electric interaction system. Simulations are conducted by varying the streamwise gap distance (G_x/L) between the flags in the tandem configuration from 0.1 to 3.2. It is found that the power coefficient of the tandem inverted flags varies with the piezoelectric tuning parameter (β). Maximum $\bar{C}_P$ occurs at $\beta = 1$ and $\beta = 1.5$ when $\alpha = 0.3$ and 0.5, respectively for the all separation distances. For both α, $\bar{C}_P$ of Flag 1 is larger than that of Flag 2 at all G_x/L because of the larger flapping amplitude. The results indicate that for $\alpha = 0.5$, $\bar{C}_P$ of Flag 1 becomes greater than that of the single flag for $1.3 < G_x/L < 2.5$ caused by the increase in the flag frequency. Results show that optimum $\bar{C}_P$ occurs at $G_x/L = 1.8$ and $\alpha = 0.5$ with $\beta = 1.5$. This is caused by the constructive interaction mode between vortices at this separation distances, increasing the flapping amplitude and frequency, and consequently the power coefficient. The energy harvesting performance of the piezoelectric flags in the side-by-side and staggered arrangements will be studied in the near future.

Acknowledgments

This research was undertaken with the assistance of resources from the National Computational Infrastructure (NCI), which is supported by the Australian Government. Soudeh Mazharmanesh wishes to gratefully acknowledge the support of the University of New South Wales Tuition Fee Scholarship for the pursuit of this study. Dr. F.-B Tian is the recipient of an Australian Research Council Discovery Early Career Research Award (project number DE160101098).

References

[1] AKAYDIN, H. D., ELVIN, N. & ANDREOPOULOS, Y. 2010. Energy harvesting from highly unsteady fluid flows using piezoelectric materials. *Journal of Intelligent Material Systems and Structures,* 21**,** 1263-1278.

[2] AKCABAY, D. T. & YOUNG, Y. L. 2012. Hydroelastic response and energy harvesting potential of flexible piezoelectric beams in viscous flow. *Physics of Fluids,* 24.

[3] DUNNMON, J. A., STANTON, S. C., MANN, B. P. & DOWELL, E. H. 2011. Power extraction from aeroelastic limit cycle oscillations. *Journal of Fluids and Structures,* 27**,** 1182-1198.

[4] HUANG, H., WEI, H. & LU, X. Y. 2018. Coupling performance of tandem flexible inverted flags in a uniform flow. *Journal of Fluid Mechanics,* 837**,** 461-476.

[5] HUANG, W. X., SHIN, S. J. & SUNG, H. J. 2007. Simulation of flexible filaments in a uniform flow by the immersed boundary method. *Journal of Computational Physics,* 226**,** 2206-2228.

[6] JIA, L. B. & YIN, X. Z. 2008. Passive oscillations of two tandem flexible filaments in a flowing soap film. *Physical Review Letters,* 100**,** 228104.

[7] KIM, D., COSSE, J., CERDEIRA, C. H. & GHARIB, M. 2013. Flapping dynamics of an inverted flag. *Journal of Fluid Mechanics,* 736**,** R1.

[8] KIM, S., HUANG, W. X. & SUNG, H. J. 2010. Constructive and destructive interaction modes between two tandem flexible flags in viscous flow. *Journal of Fluid Mechanics,* 661**,** 511-521.

[9] LIU, Z., LAI, J. C. S., YOUNG, J. & TIAN, F. B. 2017. Discrete vortex method with flow separation corrections for a flapping foil power generator. *AIAA Journal,* 55**,** 410-418.

[10] MICHELIN, S. & DOARE, O. 2013. Energy harvesting efficiency of piezoelectric flags in axial flows. *Journal of Fluid Mechanics,* 714**,** 489-504.

[11] PENG, Y., SHU, C., CHEW, Y. T., NIU, X. D. & LU, X. Y. 2006. Application of multi-block approach in the immersed boundary-lattice Boltzmann method for viscous fluid flows. *Journal of Computational Physics,* 218**,** 460-478.

[12] RISTROPH, L. & ZHANG, J. 2008. Anomalous hydrodynamic drafting of interactingfFlapping flags. *Physical Review Letters,* 101**,** 194502.

[13] SHELLEY, M. J. & ZHANG, J. 2011. Flapping and bending bodies interacting with fluid flows. *Annual Review of Fluid Mechanics,* 43**,** 449-465.

[14] SHOELE, K. & MITTAL, R. 2016. Energy harvesting by flow-induced flutter in a simple model of an inverted piezoelectric flag. *Journal of Fluid Mechanics,* 790**,** 582-606.

[15] TIAN, F.-B., LUO, H., ZHU, L., LIAO, J. C. & LU, X.-Y. 2011. An efficient immersed boundary-lattice Boltzmann method for the hydrodynamic interaction of elastic filaments. *Journal of Computational Physics,* 230**,** 7266-7283.

[16] TIAN, F. B., Wang, Y., Young, J. & Lai, J. C. S. (2015) An FSI solution technique based on the DSD/SST method and its applications, Math. Model. Meth. Appl. Sci. 25, 2257-2285.

[17] WU, J., SHU, C., ZHAO, N. & TIAN, F. B. 2015a. Numerical study on the power extraction performance of a flapping foil with a flexible tail. *Physics of Fluids,* 27**,** 013602.

[18] WU, J., WU, J., TIAN, F. B., ZHAO, N. & LI, Y. D. 2015b. How a flexible tail improves the power extraction efficiency of a semi-activated flapping foil system: A numerical study. *Journal of Fluids and Structures,* 54**,** 886-899.

[19] XU, Y. Q., JIANG, Y. Q., WU, J., SUI, Y. & TIAN, F. B. 2018. Benchmark numerical solutions for two-dimensional fluid–structure interaction involving large displacements with the deforming-spatial-domain/ stabilized space–time and immersed boundary–lattice Boltzmann methods. *Journal of Mechanical Engineering Science***,** 232, 2500-2514..

[20] ZHU, L. 2009. Interaction of two tandem deformable bodies in a viscous incompressible flow. *Journal of Fluid Mechanics,* 635**,** 455-475.